HYDROLOGICAL PROCESSES
Hydrol. Process. **24**, 136–146 (2010)
Published online 19 October 2009 in Wiley InterScience
(www.interscience.wiley.com) DOI: 10.1002/hyp.7484

A comprehensive approach to characterization of the nonlinearity of runoff in the headwaters of the Tarim River, western China

Jianhua Xu,[1]* Weihong Li,[2] Minhe Ji,[1] Feng Lu[1] and Shan Dong[1]

[1] *The Research Center for East-West Cooperation in China, The Key Lab of GIScience of the Education Ministry PRC, East China Normal University, Shanghai 200062, China*

[2] *The Key Laboratory of Oasis Ecology and Desert Environment, Xinjiang Institute of Ecology and Geography, Chinese Academy of Sciences, Urumqi, Xinjiang 830011, China*

Abstract:

Nonlinear characteristics of the runoff processes in the headwaters of the Tarim River were identified and evaluated using several selected methods, including wavelet analysis, correlation dimension, and R/S analysis. Time-series of annual data describing runoff, average temperature, and precipitation from 1957 to 2005 were used to construct and test empirical models. The primary findings of this study were as follows: (1) The annual runoff of the headwaters are complex and nonlinear in nature, and they each presented periodic, nonlinear trends at the chosen time scales, chaotic dynamics, and long-memory characteristics. (2) These nonlinear trends appeared to have resulted from the regional climatic changes that occurred during the study period. The periodicity of changes in runoff occurred on an approximately 25-year cycle, which appeared to be correlated with temperature and precipitation cycles. In addition, the annual runoff exhibited a significant, positive correlation with the temperature and precipitation factors at the 4-, 8-, 16-, and 32-year temporal scales. (3) The correlation dimensions of the attractor derived from the runoff time series for the Hotan, Yarkand, and Aksu rivers were all greater than 3·0 and non-integral, implying that all three rivers are dynamic chaotic systems that are sensitive to initial conditions, and that the dynamic modelling of their annual runoff requires at least four independent variables. (4) The computed Hurst exponents indicate that a long-term memory characteristic exists in the annual runoff processes. However, there were some differences observed, with the Aksu and Yarkand rivers demonstrating a persistent trait, and the Hotan River exhibiting an anti-persistent feature. Copyright © 2009 John Wiley & Sons, Ltd.

KEY WORDS runoff; headwater; Tarim River; nonlinearity; wavelet; correlation dimension; Hurst exponent

Received 20 May 2008; Accepted 02 September 2009

INTRODUCTION

Water shortages and related ecological degradation comprise the most pressing environmental issues in western and northwestern China (Fang *et al*., 2007). This region contains China's largest continental river basin, the Tarim River basin, which is rich in natural resources, but has a very fragile ecosystem. Water is a critical ecological element that is scarce; therefore, water is the source of great controversy in this semi-arid environment. Indeed, the distribution of water in the region has resulted in the need to determine whether to develop the local economy or to protect the fragile ecosystem, rather than balancing both. This situation has severely restricted the sustainable development of the regional economy in the Tarim River Basin (Chen *et al*., 2004; Liu and Chen, 2007).

In the last 20 years, many studies have been conducted to evaluate climatic change and the hydrological processes in the arid and semi-arid regions in northwestern China. A number of studies have indicated that there was a salient turning point in the hydrological and climatic processes of the region after the 1980s. This new trend was characterized by a continual increase in temperature and precipitation, added river runoff volumes, increased lake water surface elevation and area, and elevated groundwater levels. These changes have led to increased water resources, providing immediate relief to the local water shortage. However, the climatic change has also caused the accelerated retreat of glaciers, which are important natural water reservoirs for the delta ecosystems in inland China. This phenomenon has raised widespread concerns worldwide and recently has become a hot topic in related academic fields.

Many case studies in different countries and regions have suggested that a hydrological process is a highly complex system, with nonlinearity as its basic characteristic (Ibbitt and Woods, 2004; Liu *et al*., 2006; Strupezewski *et al*., 2006; Sivakumar, 2007; Liu, 2008; Wang *et al*., 2008). As a result, the nonlinearity of runoff processes has been explored using various nonlinear analytical methods and models, including wavelets, artificial neural networks, and the fractal theory (Wilcox *et al*., 1991; Smith *et al*., 1998; Chou, 2007; Hu *et al*., 2008; Movahed and Hermanis, 2008). However, it has proven difficult to achieve a thorough understanding of the

* Correspondence to: Jianhua Xu, The Research Center for East-West Cooperation in China, East China Normal University, 200062 Shanghai, China. E-mail: jhxu@geo.ecnu.edu.cn

Copyright © 2009 John Wiley & Sons, Ltd.

nonlinear mechanism of any individual runoff process. Specifically, there is still a lack of effective means available to reveal the type of nonlinearity underlying runoff processes and the strength of nonlinearity at different time scales. Theoretically, hydrological process can be evaluated to determine if they comprise an ordered, deterministic system, an unordered, random system, or a chaotic, dynamic system, and whether change patterns of periodicity or quasi-periodicity exist. Specific to the series of climatic changes that have occurred in the arid/semi-arid region of western China, such inquiries may be designed to determine if these changes represent a localized transition to a warm and wet climate type in response to global warming, or merely reflect a centennial periodicity in hydrological dynamics. To date, these questions have not received satisfactory answers; therefore, more studies are required to explore the nonlinear characteristics of hydrological processes from different perspectives and using different methods.

The present study is focused on the three headwaters (Hotan, Yarkand, and Aksu) of the Tarim River, which have been relatively undisturbed by human activities. To date, the nonlinear characteristics of the runoff from these headwaters are still not well understood. Therefore, several different methods were employed in this study to identify and understand the different aspects of nonlinear characteristics of the annual runoff with respect to the natural forces behind these patterns. Specifically, wavelet analyses were conducted to reveal the nonlinear trends behind the runoff processes at different time scales, a correlation dimension analysis was employed to characterize their chaotic dynamics, and the R/S analysis method was used to uncover their long-term correlation characteristics. It is hoped that the results of this study will provide new insight into the hydrological process associated with these rivers.

MATERIALS AND METHODS

Study area

The Tarim River basin covers an area of $1{\cdot}02 \times 10^6$ km^2 and is the largest continental river basin in China. The basin covers the entire southern part of Xinjiang in western China and is characterized by an abundance of rich natural resources and a fragile environment. This region has an extreme desert climate with an annual average temperature of $10{\cdot}6 \sim 11{\cdot}5\,^{\circ}$C. In addition, the monthly mean temperature ranges from 20 to 30 °C in July and -10 to $-20\,^{\circ}$C in January and the highest and lowest temperatures are $+43{\cdot}6\,^{\circ}$C and $-27{\cdot}5\,^{\circ}$C, respectively. The accumulative temperature $>10\,^{\circ}$C ranges from 4100 to 4300 °C. The average annual precipitation is approximately 116·8 mm for the entire area, with an uneven distribution of $200 \sim 500$ mm in the mountainous area, $50 \sim 80$ mm on the edges of the basin, and only $17{\cdot}4 \sim 25{\cdot}0$ mm in the central portion of the basin. There is great temporal unevenness in precipitation within each year as well. More than 80% of the total annual precipitation falls between May and September in the high-flow season, and less than 20% of the total precipitation occurs between November and April.

The main channel of the Tarim River is 1321 km in length. Naturally and historically the Tarim River basin consists of 114 rivers from nine drainage systems, which include the Aksu, Hotan, Yarkand, Qarqan, Keriya, Dina, Kaxgar, and Kaidu-Konqi Rivers. The basin contains $20{\cdot}44 \times 10^6$ ha of arable lands and has a human population of $8{\cdot}26 \times 10^6$. The mean annual natural surface runoff is $3{\cdot}98 \times 10^{10}$ m^3, most of which originates from glaciers, snowmelt, and precipitation in the surrounding mountains.

Intensive disturbances caused by human activities, particularly in response to excessive water resources exploitation, have brought about marked changes during the past 50 years. The drainage systems gradually disintegrated when the Weigan, Kaxgar, Dina, Keriya, and Qarqan rivers stopped flowing into the mainstream and were eventually disconnected from it. Today, there are only three drainage systems connected to the mainstream of the Tarim, Aksu, Yarkand, and Hotan Rivers. The Aksu River has two main tributaries (the Tongshigan and Kumalak) and originates from the Tianshan Mountains in the northwest portion of the basin. The Hotan River also has two main tributaries (the Kalaksh and Yulongkash) and originates in the Kunlun Mountains and flows through the southwestern portion of the basin. The Yarkand River originates from the Pamir Plateau and lies between the Aksu River and the Yarkand River (Figure 1).

As mentioned above, glaciers, snowmelt, and precipitation in the surrounding mountains are the major sources of runoff in the Tarim River. Specifically, glacier melt and snowmelt comprise 48·2% of the total runoff of the river. Interannual runoff variability is small, with a coefficient of variation ranging from 0·15 to 0·25 and maximum and minimum modular coefficients of 1·36 and 0·79, respectively. Additionally, seasonal runoff is unevenly distributed, with runoff during the flood season (June–August) accounting for 60%$\sim$ 80% of the total annual runoff (Chen *et al*., 2003).

Data

To evaluate the nonlinear trend in annual runoff in the three headwaters of the Tarim River, the runoff time series from 1957 to 2005 for the five sub-rivers were used. The data were obtained from the Xiehela and Shaliguilank hydrologic stations for Aksu, from the Kaqun hydrologic station for Yarkand, and from the Tonguzluok and Wuluwat hydrologic stations for Hotan. Because all stations are located in the source areas of these rivers, the amount of water used by people within each tributary basin is minimal compared to the total discharge; therefore, it was assumed that the observed hydrological records reflect the natural conditions.

Long-term climate changes can alter the runoff production pattern, the timing of hydrological events, and the

Copyright © 2009 John Wiley & Sons, Ltd.

DOI: 10.1002/hyp

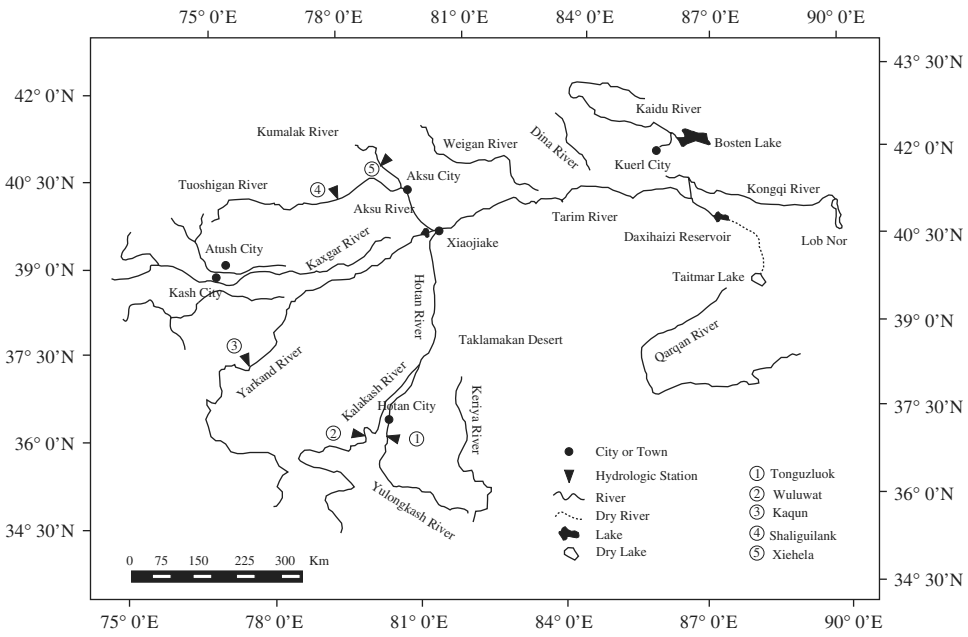

Figure 1. Location of the three headwaters of the Tarim River

frequency and severity of floods, particularly in arid or semi-arid regions. Therefore, a small change in precipitation and temperature may result in marked changes in runoff (Gan, 2000). To investigate the relationship between the runoff and the regional climate change, this study used the time series of annual average temperature and annual precipitation from 23 meteorological stations in the Tarim River Basin for the same study period.

Methodology

Three analytical tools with different perspectives were used to evaluate different temporal characteristics of the annual runoff from the Tarim River's three headwaters and their relationships with regional climatic changes. First, a wavelet transform was used to reveal the periodicity and nonlinear trend in changes in the annual runoff. This included wavelet decomposition and reconstruction to approximate the total annual runoff of the headwaters with the annual average temperature and the annual precipitation in the region over the entire study period at varying time scales. The response of the annual runoff total to climatic changes was revealed though correlation analysis. Second, the phase space reconstruction method was employed to compute correlation dimensions for attractors in an attempt to characterize the chaotic dynamics of the annual runoff process. Finally, the R/S method was applied to compute the Hurst exponent to show the long-term correlation characteristics of the annual runoff over the 49-year study period.

WAVELET ANALYSIS

Wavelet transformation has been shown to be a powerful technique for characterization of the frequency, intensity, time position, and duration of variations in climate and hydrological time series (Smith *et al*., 1998; Torrence and Compo, 1998; Chou, 2007; Xu *et al*., 2008b). Wavelet analysis can also reveal the localized time and frequency information without requiring the time series to be stationary, as required by the Fourier transform and other spectral methods.

A continuous wavelet function $\Psi(\eta)$ that depends on a nondimensional time parameter η can be written as (Labat, 2005):

$$\Psi(\eta) = \Psi(a, b) = |a|^{-1/2}\Psi(\frac{t-b}{a}) \quad (1)$$

where, t denotes time, a is the scale parameter and b is the translation parameter. $\Psi(\eta)$ must have a zero mean and be localized in both time and Fourier space (Farge, 1992). The continuous wavelet transform (CWT) of a discrete signal, $x(t)$, such as the time series of runoff, temperature, or precipitation, is expressed by the convolution of $x(t)$ with a scaled and translated $\Psi(\eta)$,

$$W_x(a, b) = |a|^{-1/2} \int_{-\infty}^{+\infty} x(t)\Psi^*(\frac{t-b}{a})\mathrm{d}t \quad (2)$$

where * indicates the complex conjugate and $W_x(a, b)$ denotes the wavelet coefficient. Thus, the concept of frequency is replaced by that of scale, which can characterize the variation in the signal, $x(t)$, at a given time scale.

The wavelet variance that is used to detect the periods present in the signal, $x(t)$, can be expressed as:

$$W_x(a) = \int_{-\infty}^{+\infty} |W_x(a, b)|^2 \mathrm{d}b \quad (3)$$

Selecting a proper wavelet function is a prerequisite for time series analysis. The actual criteria for wavelet selection include self-similarity, compactness, and smoothness

Copyright © 2009 John Wiley & Sons, Ltd.

DOI: 10.1002/hyp

(Ramsey, 1999). For the present study, symlet 8 was chosen as the wavelet function according to these criteria.

The nonlinear trend of a time series, $x(t)$, can be analysed at multiple scales through wavelet decomposition on the basis of the discrete wavelet transform (DWT). The DWT is defined taking discrete values of a and b (Banakar and Azeem, 2008). The full DWT for signal, $x(t)$, can be represented as (Mallat, 1989):

$$x(t) = \sum_k \mu_{j_0,k}\phi_{j_0,k}(t) + \sum_{j=1}^{j_0}\sum_k \omega_{j,k}\psi_{j,k}(t) \qquad (4)$$

where $\phi_{j_0,k}(t)$ and $\psi_{j,k}(t)$ are the flexing and parallel shift of the basic scaling function, $\phi(t)$, and the mother wavelet function, $\psi(t)$, and $\mu_{j_0,k}(j < j_0)$ and $\omega_{j,k}$ are the scaling coefficients and the wavelet coefficients, respectively. Generally, scales and positions are based on powers of 2, which is the dyadic DWT (Sun *et al*., 2006).

Once a mother wavelet is selected, the wavelet transform can be used to decompose a signal according to scale, allowing separation of the fine-scale behaviour (detail) from the large-scale behaviour (approximation) of the signal (Bruce *et al*., 2002). The relationship between scale and signal behaviour is designated as follows: low scale corresponds to compressed wavelet as well as rapidly changing details, namely high frequency; whereas high scale corresponds to stretched wavelet and slowly changing coarse features, namely low frequency. Signal decomposition is typically conducted in an iterative fashion using a series of scales such as $a = 2, 4, 8, \ldots\ldots, 2^{\mathrm{L}}$, with successive approximations being split in turn so that one signal is broken down into many lower resolution components.

CORRELATION DIMENSION

The correlation dimension method is usually applied to analyse a runoff series and determine if the river flow exhibits a chaotic dynamic characteristic (Sivakumar, 2007; Sivakumar and Chen, 2007; Xu *et al*., 2009). Consider $x(t)$, the time series of annual runoff, and suppose it is generated by a nonlinear dynamic system with m degrees of freedom. To restore the dynamic characteristic of the original system, it is necessary to construct an appropriate series of state vectors, $X^{(m)}(t)$, with delay coordinates in the m-dimensional phase space according to the basic ideas initiated by Grassberger and Procaccia (1983):

$$X^{(m)}(t) = \{x(t), x(t+\tau), \ldots, x(t+(m-1)\tau)\} \qquad (5)$$

where m is the embedding dimension and τ is an appropriate time delay.

The trajectory in the phase space is defined as a sequence of m-dimensional vectors. If the dynamics of the system can be reduced to a set of deterministic laws, the trajectories of the system converge towards a subset of the phase space, which is called an 'attractor'. Many natural systems do not conform with time to a cyclic trajectory. Some nonlinear dissipative dynamic systems tend to shift towards the attractors for which the motion is chaotic, i.e. not periodic and unpredictable over long times. The attractors of such systems are called strange attractors. For the set of points on the attractor, using the G-P method (Grassberger and Procaccia, 1983), the correlation-integrals are defined to distinguish between stochastic and chaotic behaviours.

The correlation-integrals can be defined as follows:

$$C(r) = \frac{1}{N_{\mathrm{R}}^2}\sum_{j=1}^{N_{\mathrm{R}}}\sum_{i=1}^{N_{\mathrm{R}}}\Theta(r - |X_i - X_j|) \qquad (6)$$

where r is the surveyor's rod for distance, N_{R} is the number of reference points taken from N, and N is the number of points, $X^{(m)}(t)$. The relationship between N and N_{R} is $N_{\mathrm{R}} = N - (m-1)\tau$. $\Theta(x)$ is the Heaviside function, which is defined as:

$$\Theta(x) = \begin{cases} 0 & x \le 0 \\ 1 & x > 0 \end{cases} \qquad (7)$$

The expression counts the number of points in the dataset that are closer than the radius, r, within a hypersphere of the radius, r, and then divides this value by the square of the total number of points (because of normalization). As $r \to 0$, the correlation exponent, d, is defined as:

$$C(r) \propto r^d \qquad (8)$$

It is apparent that the correlation exponent, d, is given by the slope coefficient of $\ln C(r)$ versus $\ln r$. According to $(\ln r, \ln C(r))$, d can be obtained by the least squares method (LSM) using a log-log grid.

To detect the chaotic behaviour of the system, the correlation exponent has to be plotted as a function of the embedding dimension (as shown in Figure 8). If the system is purely random (e.g. white noise) the correlation exponent increases as the embedding dimension increases, without reaching the saturation value.

If there are deterministic dynamics in the system, the correlation exponent reaches the saturation value, which means that it remains approximately constant as the embedding dimension increases. The saturated correlation exponent is called the correlation dimension of the attractor. The correlation dimension belongs to the invariants of the motion on the attractor. It is generally assumed that the correlation dimension equals the number of degrees of freedom of the system, and higher embedding dimensions are therefore redundant. For example, to describe the position of the point on the plane (two-dimensional system), the third dimension is not necessary because it is redundant. In addition, the correlation dimension is often fractal and represented as a nonintegral dimension, which is typical for chaotic dynamical systems that are very sensitive to initial conditions.

The correlation dimension provides information regarding the dimension of the phase–space required for embedding the attractor. It is important for determining

Copyright © 2009 John Wiley & Sons, Ltd.

DOI: 10.1002/hyp

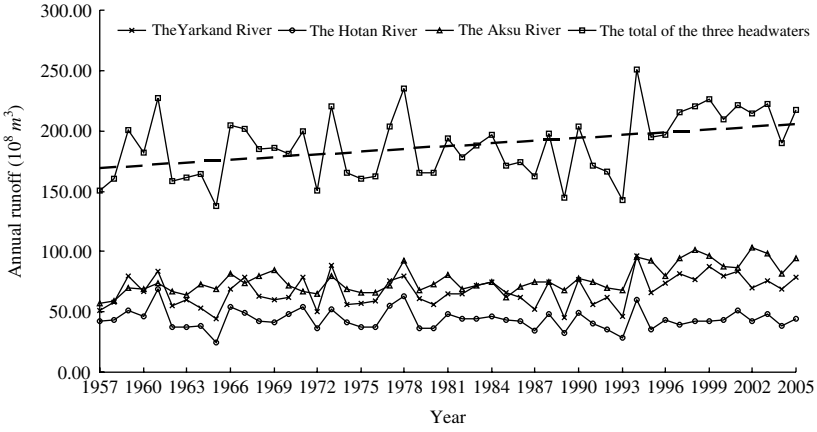

Figure 2. Individual and total annual runoff of the three headwaters of the Tarim River

the number of dimensions necessary to embed the attractor and the number of variables present in the evolution of the process.

R/S ANALYSIS METHOD

R/S analysis, which is also called rescaled range analysis, is usually applied to analyse long-term correlation characteristics of a time series (Li *et al.*, 2008; Xu *et al.*, 2008b). The principle of R/S analysis is briefly introduced as follows (Mandelbrot and Wallis, 1969; Turcotte, 1997):

Considering a time series $x(t)$, such as the annual runoff sequence of a certain river, for any positive integer $\tau \geq 1$, the mean value series is defined as:

$$\langle x \rangle_\tau = \frac{1}{\tau} \sum_{t=1}^{\tau} x(t) \quad \tau = 1, 2, \ldots \tag{9}$$

The accumulative deviation is:

$$X(t, \tau) = \sum_{u=1}^{t} (x(u) - \langle x \rangle_\tau) \qquad 1 \leq t \leq \tau \tag{10}$$

The extreme deviation is:

$$R(\tau) = \max_{1 \leq t \leq \tau} X(t, \tau) - \min_{1 \leq t \leq \tau} X(t, \tau) \quad \tau = 1, 2, \ldots \tag{11}$$

The standard deviation is:

$$S(\tau) = \left[\frac{1}{\tau} \sum_{t=1}^{\tau} (x(t) - \langle x \rangle_\tau)^2 \right]^{\frac{1}{2}} \quad \tau = 1, 2, \ldots \tag{12}$$

When analysing the statistic rule of $R(\tau)/S(\tau) \underset{=}{\Delta} R/S$, H E Hurst discovered a relational expression,

$$R/S \propto (\frac{\tau}{2})^H \tag{13}$$

which can be used to identify the Hurst phenomenon in the time series, where H is known as the Hurst exponent. It is evident that H is given by the slope coefficient of R/S versus $\tau/2$. According to $(\ln \tau/2, \ln(R/S))$, H can be obtained by the LSM in a log-log grid.

Hurst *et al.* (1965) once demonstrated that if $x(t)$ is an independently random series with limited variance, the exponent, $H = 0{\cdot}5$, and H $(0 < H < 1)$ is dependent on a correlation function $C(t)$:

$$C(t) = 2^{2H-1} - 1 \tag{14}$$

When $H > 0{\cdot}5$ and $C(t) > 0$, the process has a long, enduring characteristic, and the future trend of the time series will be consistent with the past. In other words, if the past showed an increasing trend, the future will also show an increasing trend. When $H < 0{\cdot}5$ and $C(t) < 0$, the process has an anti-persistence characteristic, and the future trend of the time series will be opposite from the past. In other words, if the past showed an increasing trend, the future will assume the reducing trend. When $H = 0{\cdot}5$ and $C(t) = 0$, the process is stochastic; in other words, there is no correlation or only a short-range correlation in the process (Ai and Li, 1993).

RESULTS AND DISCUSSION

Nonlinear trend of annual runoff

The raw data associated with the annual runoff time series of the individual headwaters as well as the combined data resulted in a fluctuating pattern for the period of 1957–2005 (Figure 2). However, it is difficult to identify any trends (e.g. periodicity) simply based on the surface of the oscillation pattern. This issue was addressed here using a CWT.

Based on symlet 8, which was selected according to the criteria of self-similarity, compactness, and smoothness (Ramsey, 1999), the CWT was applied to the annual runoff time series of the three headwaters separately and combined. The computed wavelet variances (Figure 3) indicate that the runoff series for Aksu and Yarkand, as well as the combined data for the three headwaters, were all locally maximized in the 25th year, whereas for Hotan, the local maximum occurred in the 24th year. These results imply that there was a 25-year cycle for

Copyright © 2009 John Wiley & Sons, Ltd.

DOI: 10.1002/hyp

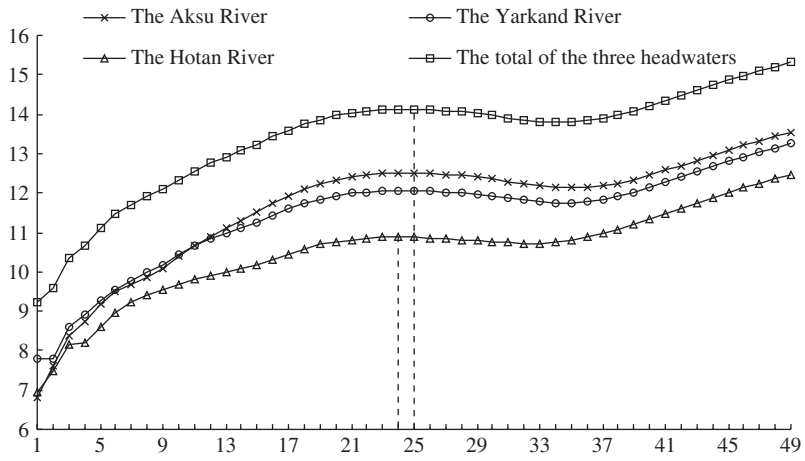

Figure 3. Wavelet variances of annual runoff of the three headwaters of the Tarim River

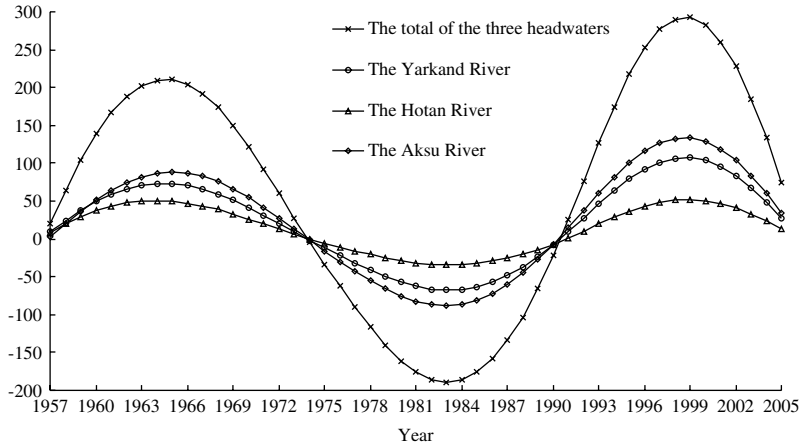

Figure 4. Wavelet coefficients for the annual runoff of the three headwaters of the Tarim River at the time scale of 25 years

Aksu and Yarkand and a 24-year cycle for Hotan over the study period of 1957–2005, which represents a periodic pattern concealed in the temporal fluctuation of the runoff of the three headwaters.

The wavelet coefficients computed from the time-series annual runoff on a 25-year time scale revealed that there was a water surplus and deficit situation for the individual headwaters as well as the combined headwaters. The years 1974 and 1990 served as breakpoints separating two water-surplus periods from one water-deficit period. Specifically, the wavelet coefficients for the period of 1957–1974 were all greater than zero, indicating the presence of a water surplus in the three headwaters. The wavelet coefficients for the period from 1974 to 1990 were all less than zero, implying a deficit in water in the headwaters. The coefficient values from 1990 to 2005 became greater than zero again, suggesting a new water-surplus period (Figure 4).

Some studies have shown that stream flows can also be influenced by other variables (called exogenous variables in time series analysis), such as matter and energy, and that such influences might not be constants (Chen and Kumar, 2004; Shao *et al.*, 2009). It is important to identify possible causes for the occurrence of such periodic runoff patterns in the three headwaters in this system. It is well known that the mainstream Tarim River is an inland river located in the arid/semi-arid western China that does not generate any volume. Indeed, its runoff primarily comes from its three headwaters, which are in turn fed by mountain snowmelt and regional precipitation. Therefore, the dynamics of regional climate, especially temperature and precipitation, directly affect the annual changes in the runoff of the headwaters. For this reason, it is important to determine if there is a similar cyclic pattern in the time series of annual average temperature and annual precipitation in the Tarim basin during the study period. Accordingly, the wavelet variances were used to explore these two climate factors, and the computed results are presented in Figure 5.

The wavelet variance curves show a local maximum in the 24th year for temperature and in the 26th year for precipitation, which suggests the existence of a 24-year and a 26-year cycle for the respective climate factors. A visual comparison of Figures 3 and 4 seems to suggest a close fit between the runoff series and the climate factors. In addition, their periodicities are both around 25 years. These findings suggest that temporal variations in the annual runoff of the headwaters might be properly explained by the regional climatic changes.

Copyright © 2009 John Wiley & Sons, Ltd.

DOI: 10.1002/hyp

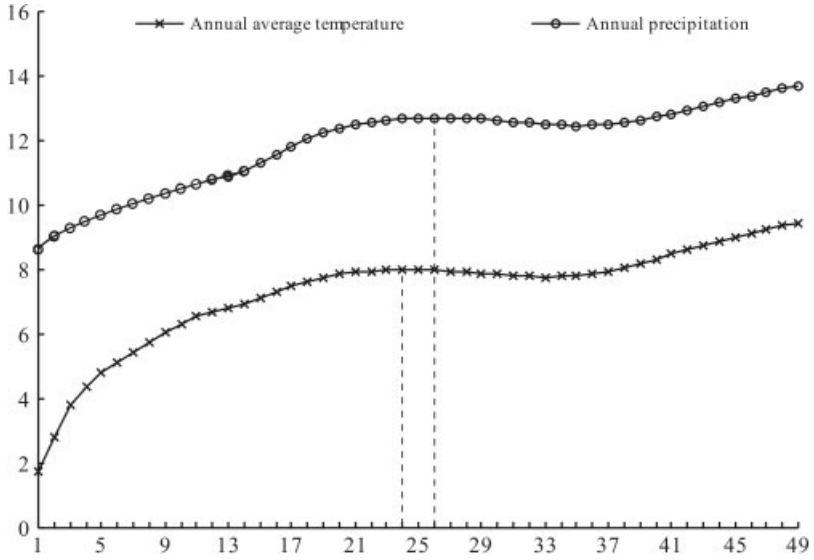

Figure 5. Wavelet variances of annual average temperature and annual precipitation in the Tarim River basin

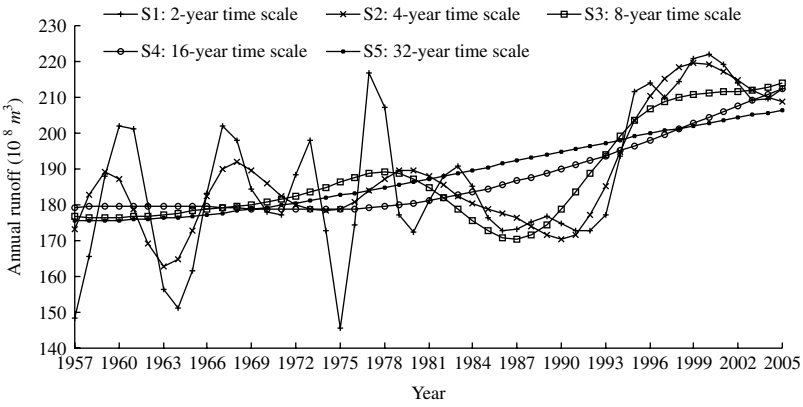

Figure 6. Wavelet approximations for the total annual runoff of the three headwaters at different time scales

To further verify this relationship, the following linear regression model was developed using the temperature and precipitation time series as two independent variables and the total runoff of the three headwaters as the independent variable:

$$AR = 22{\cdot}7735AAT - 0{\cdot}0825AP - 27{\cdot}4592 \quad (15)$$
$$R^2 = 0{\cdot}2338;\ F = 7{\cdot}0194;\ \alpha = 0{\cdot}01$$

where AR denotes the annual runoff, AAT is the annual average temperature, and AP represents the annual precipitation.

The test results showed that the above regression was significant at $\alpha = 0{\cdot}01$. Furthermore, Equation (15) revealed a positive correlation between the combined runoff of all three headwaters and the temperature factor, which was expected. These results are readily supported by the fact that the majority of water supplied to the headwaters comes from glacial melt and snow melt, which have been occurring at increased rates as the temperature in the region increases. These results have been confirmed by other studies (Wang *et al*., 2006). However, Equation (15) also indicates the existence of a weak, negative correlation between the annual total runoff and the annual precipitation in the region, which does not seem reasonable. Indeed, this finding conflicts with the results of other studies (Chen and Xu, 2005; Chen *et al*., 2006), which have suggested that both the temperature and precipitation series in the Tarim basin have been increasing in a pattern similar to that of annual runoff over the past 50 years. It is possible that this inconsistency is caused by noise in the raw time-series data, which should be filtered out via wavelet decomposition based on the DWT (Xu *et al*., 2008a).

The wavelet decomposition of the time series runoff total at five time scales resulted in five variants of nonlinear trends (Figure 6). These five time scales are designated as S1 through S5 and started from 2 years (S1), then increased by twofold for the next scale level until a 32-year time scale was attained (S5).

Figure 6 provides a good device of comparing the results filtered at different time scales. The S1 curve retains a large amount of residual noise from the raw data (see Figure 2 for a comparison), and drastic fluctuations along the entire time span. These characteristics indicate

Copyright © 2009 John Wiley & Sons, Ltd.

DOI: 10.1002/hyp

Table I. Regression equations describing the relationship between annual runoff and annual average temperature and annual precipitation at different time scales

Time scale	Regression equation	R^2	F	Significance level α
S1	$AR = 24{\cdot}3728AAT - 0{\cdot}0618AP - 44{\cdot}6754$	0·3606	12·9728	0·001
S2	$AR = 20{\cdot}037AAT + 0{\cdot}1383AP - 19{\cdot}12$	0·4572	19·3749	0·001
S3	$AR = 26{\cdot}7059AAT + 0{\cdot}1217AP - 83{\cdot}3285$	0·7198	59·0842	0·001
S4	$AR = 14{\cdot}4302AAT + 0{\cdot}4692AP + 7{\cdot}0097$	0·9530	466·3466	0·001
S5	$AR = 17{\cdot}1003AAT + 0{\cdot}3933AP - 11{\cdot}6140$	0·9957	5302·3256	0·001

Notes: AR, annual runoff; AAT, annual average temperature; AP, annual precipitation; S1, S2, S3, S4, and S5 represent 2-, 4-, 8-, 16-, and 32-year time scales, respectively.

that, although the total runoff from the headwaters varied greatly throughout the study period, there was a hidden increasing trend. The S2 curve still retains a considerable amount of residual noise, as indicated by the presence of four peaks and three valleys. However, the S2 curve is much smoother than the S1 curve, which allows the hidden increasing trend to be more apparent. The S3 curve retained much less residual noise, as indicated by the presence of only one peak and one valley. Compared to S2, the increase in runoff over time was more apparent in S3. Finally, the increasing trend becomes even more obvious in the S4 curve, whereas the S5 curve presents a nondoubtable ascending tendency.

The covariability between runoff and climate factors at multiple time scales can be examined via regression analysis based on the results of wavelet decomposition (Xu *et al*., 2008a). Using the method of wavelet decomposition described above, nonlinear trends regarding the annual average temperature and annual precipitation series were first detected and then fitted to the trends of the runoff total at different time scales through regression analysis.

The tabulated results (Table I) indicate that each regression model was statistically significant at $\alpha = 0{\cdot}001$. Table II shows the statistical tests of partial regression coefficients in different regression equations. Obviously, the regression at S1 led to an unreasonable result similar to that produced by Equation (15). This was likely due to the considerable amount of residual noise that remained from the raw data. However, the regression models produced by S2 through S5 yielded meaningful explanations in which the annual runoff was positively correlated with the annual average temperature and annual precipitation. Furthermore, the regression models revealed a stronger relationship (i.e. a greater value for their partial regression coefficient with high statistical significance) between runoff and temperature than between runoff and precipitation. These results provide further evidence supporting the view that the nonlinear ascending trend of the annual runoff time series of the three Tarim headwaters is strongly influenced by regional climate change.

Table II. Statistical tests of partial regression coefficients in each regression equation

Time scale	T			Sig.		
	Constant	*AAT*	*AP*	Constant	*AAT*	*AP*
S1	−0·9769	4·8844	−0·4373	0·3337	0·0000	0·6640
S2	−0·4713	3·9068	0·7322	0·6397	0·0003	0·4678
S3	−1·8953	4·5525	0·6521	0·0644	0·0000	0·5176
S4	0·3937	5·8403	5·6918	0·6956	0·0000	0·0000
S5	−0·3300	3·0177	1·6494	0·7429	0·0041	0·1059

The chaotic dynamics of annual runoff

Correlation dimension analysis can exhibit a chaotic dynamic characteristic of river flows (Sivakumar, 2007). This paper employed the correlation dimension to demonstrate the dynamic characteristics of the runoff time series of three headwaters. The annual runoff time series of the Aksu River was used to reconstruct the phase space, while the correlation dimension of the attractor was calculated. Different values for the radius, r, were first selected to compute the values of the correlation-integrals, $C(r)$, which were used to plot the curves within a dual logarithmic coordinate system (Figure 7). This diagram shows the relationship between $\ln C(r)$ and $\ln (r)$ for the annual runoff with a number of different embedding dimensions, m. The slope coefficient of $\ln C(r)$ versus $\ln r$, i.e. the correlation exponent, d, which was used to embed dimension $m = 1, 2, \ldots$, was calculated using the LSM.

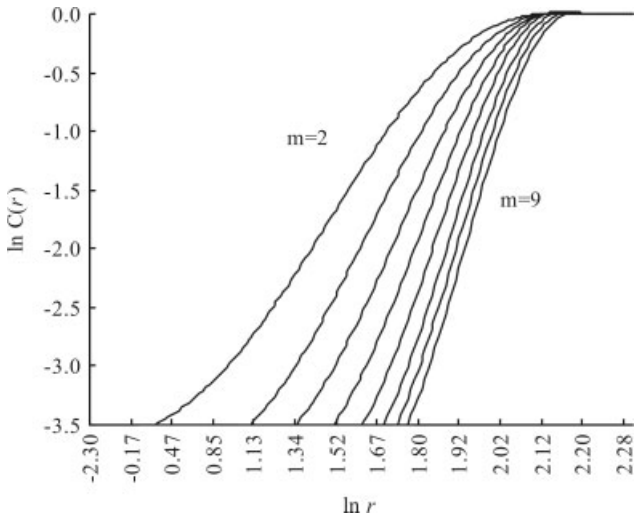

Figure 7. A plot of ln C(r) versus ln (r)

Copyright © 2009 John Wiley & Sons, Ltd.

DOI: 10.1002/hyp

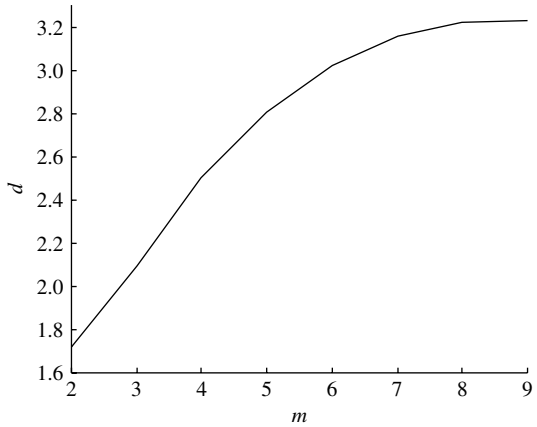

Figure 8. The correlation exponent (d) versus embedding dimension (m)

Table III. The correlation dimensions for the annual runoff processes in the three headwaters of the Tarim River

Rivers	Aksu River	Yarkand River	Hotan River
Embedding dimension (m)	7	7	7
Attractor dimension (D)	3·2092	3·2118	3·2227

Figure 8 shows the gradual saturation process of the correlation exponent. It is evident that the correlation exponent increases with embedding dimension, m, and a saturated correlation exponent, the correlation dimension of attractor (D), was obtained when $m \geq 7$.

The same procedure was used to derive the correlation dimensions of the attractors for the Yarkand and the Hotan Rivers. The index values of all three headwaters are shown in Table III. The fact that none of the correlation dimensions is an integer indicates that the annual runoff time series of all three headwaters are chaotic dynamic systems that are very sensitive to the initial conditions. Because the value of the index is above 3 for all headwaters, at least four independent variables are needed to describe the dynamics of the annual runoff process in each river.

The long-memory characteristic of annual runoff process

All statistical methods used for time series analysis are based on the assumption that all data from a given time series are independent (i.e. conforming to the Gauss distribution); hence, the series is stochastic. When Hurst (1951) and Hurst *et al*. (1965) analysed the water level of the Nile River, he found that time-series variables such as the river water level did not exhibit the stochastic characteristic, but instead showed the characteristic of durability. Based on the empirical findings of Hurst *et al*. (1965), Mandelbrot and Wallis (1968) led to a breakthrough regarding fundamental theories of traditional statistical methods. Specifically, they found that many time series no longer presented a random Brownian movement unrelated to the past, but instead showed a characteristic of long-term correlation (Comte and Renault, 1996), which he called 'fractal'.

Table IV. Hurst exponents for the annual runoff processes in the three headwaters of the Tarim River

River Name	Aksu River	Yarkand River	Hotan River
H	0·6991	0·5113	0·4367
C(t)	0·3178	0·0158	−0·0840

This study employed the rescaled range (R/S) analysis method to characterize the fractal of annual runoff processes in the three headwaters of the Tarim River. Using the R/S analysis method, the Hurst exponent (H) and the correlation function ($C(t)$) were computed for the annual runoff time series of each headwater during the period of 1957 $\sim$ 2005 (Table IV).

The results shown in Table IV suggest that the annual runoff time series for each of the Tarim's headwaters possess the characteristic of long memory. The only difference among the headwaters is that the Aksu and Yarkand Rivers demonstrate the persistent trait, whereas Hotan shows the anti-persistent feature. The H values for the Aksu and Yarkand Rivers are greater than 0·5 and the C(t) values are greater than 0, which indicate that the future tendency of the annual runoff associated with these systems is consistent with the past runoff. However, the H value is less than 0·5 and the C(t) value is less than 0 for the Hotan River, which implies that the future tendency of annual runoff is opposite to that of the past.

The results of this study cannot provide an explanation for the difference between the long-correlation characteristics of Hotan and the other two headwaters. However, the results of this study imply that the nonlinear characteristic of the annual runoff of these headwaters occurs not only along the time dimension, but also spatially. Other relevant studies (Chen *et al*., 2006; Zhang *et al*., 2007; Hao *et al*., 2008; Xu *et al*., 2008a) also confirm that the temporal pattern of annual runoff in Hotan differed from that of the other two headwaters over the last 50 years. Chen *et al*. (2006) suggested that this difference was likely related to the different geographical settings of the headstreams. However, additional studies are necessary to provide a deeper understanding of this phenomenon.

CONCLUSIONS

Experience dictates that observation from multiple angles is necessary to develop a complete picture of a polyhedron with irregular facets, which can lead to difficulties in identifying the relationship between the geometric parameters (i.e. perimeter, surface area, curvature, normal, etc.) among facets. The three headwaters of Tarim comprise a complicated system, with a level of complexity, that is much higher than that of an irregularly shaped polyhedron. The present study employed several different methods to analyse the annual runoff of these headwaters, and the results led to a few recognizable conclusions. Due to the complexity of the phenomena evaluated here, as well as the limitations of this study, it

Copyright © 2009 John Wiley & Sons, Ltd.

DOI: 10.1002/hyp

is difficult to connect the results obtained using different analytic approaches employed in this study. Nevertheless, these results provide valuable information that provides a better understanding of the nonlinear characteristics of the hydrological process of the headwaters from different angles.

The conclusions of this study include the following:

1. The hydrological processes of the three headwaters of the Tarim River, which are represented by the annual runoff time series over the 49 years considered in the study, are complex, nonlinear systems. Specifically, these processes each have certain periodic, nonlinear trends at the selected time scales, as well as chaotic dynamics, and long-memory characteristics.
2. A cyclic period of 24–25 years was detected in the annual runoff time series of the three headwaters of the Tarim River, while cyclic periods of 24 and 26 years were detected in the annual average temperature and annual precipitation, respectively. Therefore, the cyclic patterns of the runoff and the regional climate factors are in agreement (about 25 years). These results suggest that the periodicity of the annual runoff of the headwaters is the result of regional climatic changes.
3. The nonlinear runoff pattern of the three headwaters was found to be scale-dependent with respect to time. The runoff time series varied greatly at a smaller time scale (2 years), without showing any salient trend. However, analyses conducted at a wider time interval (e.g. 16 or 32 years) revealed an increasing tendency. Furthermore, the runoff and the climate factors were significantly and positively correlated at 4-, 8-, 16-, and 32-year time scales, indicating again that the nonlinear variation in annual runoff might have resulted from regional climate changes.
4. The correlation dimension of the attractor computed from the annual runoff time series was 3·2227, 3·2118, and 3·2092 for Hotan, Yarkand, and Aksu, respectively, and none of these values were integral. These results indicate that the hydrological processes in all three headwaters of the Tarim River are chaotic dynamic systems that are very sensitive to initial conditions. Since all three calculated correlation dimensions were greater than three, at least four independent variables are required to describe the dynamics of the annual runoff process in each river.
5. The Hurst exponents indicate that a long-term memory characteristic exists in the annual runoff processes. The Hurst exponents for the Aksu and Yarkand Rivers were found to be greater than 0·5, implying that the future tendency of annual runoff is consistent with those of the past. However, the Hurst exponent for the Hotan River was found to be less than 0·5, which implies that the future tendency of annual runoff is opposite to that of the past.

Based on the results of this study, the headwaters of the Tarim River comprise a highly complex geographical system. The complexity is represented by the nonlinear characteristic of their runoff processes with regard to their time-scale dependency, long-term memory, chaotic dynamics, and spatial variability. However, development of a more detailed understanding of this system will require further studies conducted using different methods and including other factors.

ACKNOWLEDGEMENTS

This work was financially supported by the Knowledge Innovation Project from the Chinese Academy of Sciences (KZCX2-XB2-03 and KZCX2-YW-127), and the Natural Science Foundation of China (40 671 014). The authors are extremely grateful to Professor Yaning Chen for his kind support and help.

REFERENCES

Ai NS, Li HQ 1993. The nonlinear science methods for Quaternary studies (in Chinese). *Quaternary Research* **13**(2): 109–120.

Banakar A, Azeem MF. 2008. Artificial wavelet neuro-fuzzy model based on parallel wavelet network and neural network. *Soft Comput* **12**: 789–808. DOI: 10.1007/s00500-007-0238-z.

Bruce LM, Koger CH, Li J. 2002. Dimensionality reduction of hyperspectral data using discrete wavelet transform feature extraction. *IEEE Transactions on Geoscience and Remote Sensing* **40**(10): 2331–2338. DOI: 10.1109/TGRS.2002.804721.

Chen J, Kumar P. 2004. A Modeling Study of the ENSO Influence on the Terrestrial Energy Profile in North America. *Journal of Climate* **17**: 1657–1670. DOI: 10.1175/1520-0442(2004)017<1657:AMSOTE>2.0.CO;2.

Chen YN, Li WH, Chen YP, Zhang HF. 2003. Water resources and ecological problems in Tarim River Basin, Xinjiang, China. In *Water and Environmental Management*, Wilderer PA, Zhu J, Schwarzenbeck N (eds). IWA Publishing: London; 3–12.

Chen YN, Takeuchi K, Xu CC, Chen YP, Xu ZX. 2006. Regional climate change and its effects on river runoff in the Tarim Basin, China. *Hydrological Processes* **20**: 2207–2216. DOI: 10.1002/hyp.6200.

Chen YN, Xu ZX. 2005. Plausible impact of global climate change on water resources in the Tarim River Basin. *Science in China (D)* **48**(1): 65–73. DOI: 10.1360/04yd0539.

Chen YN, Zhang XL, Li WH, Zhang YM. 2004. Analysis on the ecological benefits of the stream water conveyance to the dried-up river of the lower reaches of the Tarim River, China. *Science in China (D)* **47**(11): 1053–1064. DOI: 10.1360/03yd0101.

Chou CM. 2007. Efficient nonlinear modeling of rainfall-runoff process using wavelet compression. *Journal of Hydrology* **332**: 442–455. DOI:10.1016/j.jhydrol.2006.07.015.

Comte F, Renault E. 1996. Long memory continuous time models. *Journal of Econometrics* **73**(1): 101–149.

Fang CL, Bao C, Huang JC. 2007. Management implications to water resources constraint force on socio-economic system in rapid urbanization: a case study of the Hexi Corridor, NW China. *Water Resource Management* **21**: 1613–1633. DOI: 10.1007/s11269-006-9117-0.

Farge M. 1992. Wavelet transforms and their applications to turbulence. *Annual Review of Fluid Mechanics* **24**: 395–457. DOI:10.1146/annurev.fl.24.010192.002143.

Gan TY. 2000. Reducing vulnerability of water resources of Canadian Prairies to potential droughts and possible climate warming. *Water Resources Management* **14**(2): 111–135. DOI: 10.1023/A:1008195827031.

Grassberger P, Procaccia I. 1983. Characterization of strange attractor. *Physical Review Letters* **50**(5): 346–349.

Hao XM, Li WH, Chen YN, Li C. 2008. Human activity and climate factors impacting the annual runoff in the mainstream of the Tarim River (in Chinese). *Progress in Nature Science* **18**(12): 1409–1416.

Hu CH, Hao YH, Yeh TCJ, Pang B, Wu ZN. 2008. Simulation of spring flows from a karst aquifer with an artificial neural network. *Hydrological Processes* **22**: 596–604. DOI: 10.1002/hyp.6625.

Hurst HE. 1951. Long-term storage capacity of reservoirs. *Transactions of American Society of Civil Engineers* **116**: 770–808.

Copyright © 2009 John Wiley & Sons, Ltd.

Hurst HE, Black RP, Simaike YM. 1965. *Long-term Storage: An Experimental Study*. Constable: London; 1–155.

Ibbitt R, Woods R. 2004. Re-scaling the topographic index to improve the representation of physical processes in catchment models. *Journal of Hydrology* **293**: 205–218. DOI:10.1016/j.jhydrol.2004.01.016.

Labat D. 2005. Recent advances in wavelet analyses: Part 1. A review of concepts. *Journal of Hydrology* **314**: 275–288.

Li ZL, Xu ZX, Li JY, Li ZJ. 2008. Shift trend and step changes for runoff time series in the Shiyang River basin, northwest China. *Hydrological Processes* **22**: 4639–4646. DOI: 10.1002/hyp.7127.

Liu CM. 2008. The Impact of Climate change on hydrological process and water resource. *Impact of Science on Society* **2**: 21–27. in Chinese).

Liu YB, Chen YN. 2007. Saving the "Green Corridor": recharging groundwater to restore riparian forest along the lower Tarim River, China. *Ecological Restoration* **25**(2): 112–117. DOI: 10.3368/er.25.2.112.

Liu YB, Corluy J, Bahremand A, De Smedt F, Poorova J, Velcicka L. 2006. Simulation of runoff and phosphorus transport in a carpathian catchment, Slovakia. *River Research and Applications* **22**(9): 1009–1022. DOI: 10.1002/rra.953.

Mallat SG. 1989. A theory for multiresolution signal decomposition: the wavelet representation. *IEEE Transactions Pattern Analysis and Machine Intelligence* **11**(7): 674–693.

Mandelbrot BB, Wallis JR. 1968. Noah, Joseph and operational hydrology. *Water Resources Research* **4**(5): 909–918.

Mandelbrot BB, Wallis JR. 1969. Robustness of the rescaled range R/S in the measurement of noncyclic long-run statistical dependence. *Water Resources Research* **5**(5): 967–988.

Movahed MS, Hermanis E. 2008. Fractal analysis of river flow fluctuations. *Physica A: Statistical Mechanics and its Applications* **387**: 915–932. DOI: 10.1016/j.physa.2007.10.007.

Ramsey JB. 1999. Regression over timescale decompositions: a sampling analysis of distributional properties. *Economic Systems Research* **11**(2): 163–183.

Shao QX, Wong H, Li M, Ip WC. 2009. Streamflow forecasting using functional-coefficient time series model with periodic variation. *Journal of Hydrology* **368**: 88–95. DOI:10.1016/j.jhydrol.2009.01.029.

Sivakumar B. 2007. Nonlinear determinism in river flow: prediction as a possible indicator. *Earth Surface Processes and Landforms* **32**(7): 969–979. DOI: 10.1002/esp.1462.

Sivakumar B, Chen J. 2007. Suspended sediment load transport in the Mississippi River basin at St. Louis: Temporal scaling and nonlinear determinism. *Earth Surface Processes and Landforms* **32**: 269–280. DOI: 10.1002/esp.1392.

Smith LC, Turcotte DL, Isacks BL. 1998. Streamflow characterization and feature detection using a discrete wavelet transform. *Hydrological Processes* **12**: 233–249. DOI: 110.1002/(SICI)1099-1085(199802)12:2<233::AID-HYP573>3.0.CO;2–3.

Strupezewski WG, Singh VP, Weglarczyk S, Kochanek K, Mitosek HT. 2006. Complementary aspects of linear flood routing modelling and flood frequency analysis. *Hydrological Processes* **20**: 3535–3554. DOI: 10.1002/hyp.6149.

Sun GM, Dong XY, Xu GD. 2006. Tumor tissue identification based on gene expression data using DWT feature extraction and PNN classifier. *Neurocomputing* **69**: 387–402. DOI:10.1016/j.neucom.2005.04.005.

Torrence C, Compo GP. 1998. A practical guide to wavelet analysis. *Bulletin of the American Meteorological Society* **79**(1): 61–78.

Turcotte DL. 1997. *Fractals and Chaos in Geology and Geophysics*, 2nd edn. Cambridge University Press: New York; 158–162.

Wang W, Chen X, Shi P, van Gelder PHAJM. 2008. Detecting changes in extreme precipitation and extreme streamflow in the Dongjiang River Basin in southern China. *Hydrology and Earth System Sciences* **12**: 207–221.

Wang X, Xie ZC, Liu SY, Shangguan DH, Tao JJ, Yang YL. 2006. Prediction on the variation trend of glacier system in the source region of Tarim river responding to climate change (in Chinese). *Journal of Mountain Science* **24**(6): 641–646.

Wilcox BP, Seyfried MS, Matison TH. 1991. Searching for chaotic dynamics in snowmelt runoff. *Water Resources Research* **27**(6): 1005–1010. DOI: 10.1029/91WR00225.

Xu JH, Chen YN, Ji MH, Lu F. 2008a. Climate change and its effects on runoff of Kaidu River, Xinjiang, China: A multiple time-scale analysis. *Chinese Geographical Science* **18**(4): 331–339. DOI: 10.1007/s11769-008-0331-y.

Xu JH, Chen YN, Li WH, Dong S. 2008b. Long-term trend and fractal of annual runoff process in mainstream of Tarim river. *Chinese Geographical Science* **18**(1): 77–84. DOI: 10.1007/s11769-008-0077-6.

Xu JH, Chen YN, Li WH, Ji MH, Dong S. 2009. The complex nonlinear systems with fractal as well as chaotic dynamics of annual runoff processes in the three headwaters of the Tarim River. *Journal of Geographical Sciences* **19**(1): 25–35. DOI: 10.1007/s11442-009-0025-0.

Zhang XW, Shen B, Huang LM. 2007. Study on the variation law of the annual runoff in Hotan river (in Chinese). *Journal of Natural Resources* **22**(6): 974–979.

Copyright © 2009 John Wiley & Sons, Ltd.